Torsional shear strength and elastic properties of adhesively bonded glass-to-steel components

Materials and Design 192 (2020) 108739

Contents lists available at ScienceDirect

Materials and Design

journal homepage: www.elsevier.com/locate/matdes

Torsional shear strength and elastic properties of adhesively bonded glass-to-steel components

Stefano De La Pierre [a,*], Tommaso Scalici [b], Peter Tatarko [c], Antonino Valenza [b], Luca Goglio [d], Davide S. Paolino [d], Monica Ferraris [a]

[a] Department of Applied Science and Technology (DISAT), Politecnico di Torino, Italy
[b] Department of "Ingegneria Civile, Ambientale, Aerospaziale, dei Materiali" (DICAM), University of Palermo, Italy
[c] Institute of Inorganic Chemistry, Slovak Academy of Sciences, Bratislava, Slovakia
[d] Department of Mechanical and Aerospace Engineering (DIMEAS), Politecnico di Torino, Italy

HIGHLIGHTS

- Epoxy adhesive joining of soda-lime glass to AISI304 steel components
- Pure shear strength measurement: from small samples to full-scale structures
- Torsion test compared to asymmetric four-point bending
- Modelling the ductile-brittle behaviour of adhesive joints

GRAPHICAL ABSTRACT

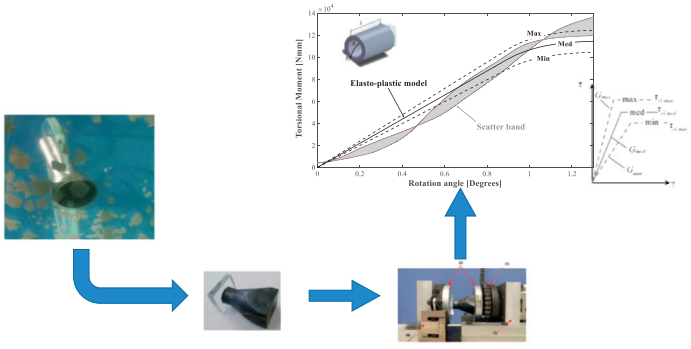

ARTICLE INFO

Article history:
Received 5 March 2020
Received in revised form 16 April 2020
Accepted 17 April 2020
Available online 28 April 2020

Keywords:
Adhesive joining
Glass
Steel
Torsion
Shear
Nano-indentation

ABSTRACT

Nowadays glass is widely used in building applications and coupled to steel through adhesive joining. Reliable mechanical characterization of these joints is necessary to design and predict the final structure performance.
In this framework, the aim of this paper is to measure the pure shear strength and elastic modulus for design and modelling of adhesive joined glass-to-steel structures.
Torsional shear strength and elastic properties of an adhesively bonded glass-to-steel component were measured on several joined steel-to-steel and steel-to-glass samples.
An epoxy resin-based adhesive was used as joining material for AISI304 steel and soda-lime glass.
The same steel and adhesive were used to obtain steel-to-steel joined sample bars to be tested in asymmetrical four-point bending, for comparison purposes.
The indentation elastic modulus of the adhesive, both inside the joined region and as a bulk, was measured by nano-indentation and impulse excitation technique.
Finally, the effect of etching on the glass was studied and correlated to the glass-steel joint strength.
This study shows that torsion test can be used to provide reliable shear strength values for design and modelling glass-to-steel adhesive joined components.

* Corresponding author.
E-mail address: stefano.delapierre@polito.it (S. De La Pierre).

https://doi.org/10.1016/j.matdes.2020.108739

1. Introduction

Glass as building material offers several unparalleled advantages with respect to other materials, such as: durability, unlimited aesthetic options, and transparency coupled with good stiffness and strength [1]. Nevertheless, the possibility to fully exploit its advantages in primary load-carrying structures (e.g. floors, facades, columns etc.) strictly depends on the combination with other structural elements made of other common materials such as steel [2].

Mechanical joints are usually used to attach glass panels to the load-bearing structure. However, the discontinuities caused by the holes as well as the drilling process may induce cracks and/or residual stresses in the glass. Fiore et al. [3] have recently shown that holes induce local stress concentration that can cause the premature failure, thus leading to safety concerns, oversized structures and the need of accurate and expensive monitoring program able to prevent fatigue failures.

To overcome these problems, adhesive joining techniques are preferred, in order to guarantee structural continuity, a more efficient and homogeneous load transmission between different elements of the structure, and to lower or suppress the stress concentration [4,5]. Moreover, adhesive joints can contribute to cost and weight saving due to their higher strength-to-weight ratio, better fatigue behaviour and ease of application. Notwithstanding the advantages presented above, the applications are still limited due to their sensitivity to manufacturing defects, harsh conditions and to difficulties in the assessment of their mechanical behaviour [6,7].

In the particular context of mechanical behaviour, several different tests have been proposed for the shear strength characterization of joined components, such as lap shear [8], modified transverse crack tensile [9], end-notched flexure [10] and end-loaded split tests [11]. However, all these tests evaluate different in-plane and out-of-plane shear failure modes or a combination of them and therefore they do not effectively measure the pure shear strength of a joined component.

Moreover, all lap shear tests should, in general, be used for comparative studies only and not to provide the shear strength of joined components for design purposes: it is worth noticing that ASTM D905-08 [12] has a *caveat* on the use of lap joint tests.

Also loading rate and strain-rate effects may significantly influence the shear strength of the joint and they should be considered for dynamic applications where the joint is subject to rapidly varying loading conditions [13,14].

The only available standard to measure the (non-lap) shear strength of joined (*ceramic*) samples is the asymmetric four-point bending (A4PB) test (ASTM C1469) [15]. This test was designed to give pure shear loading and zero bending moment in the joined area. However, Ferraris et al. [16] pointed out the difficulty of performing this test in a correct manner, because: (a) joined samples for this test should not be prepared one by one; (b) even a slight misalignment provides unreliable results; (c) if the joint bending strength is higher than 50% of the non-joined material, this test cannot be used.

Torsion tests on hourglass shaped joined components have been proposed by some authors of this paper and used by several other research groups to obtain the pure shear strength of joined samples [16–21]. If correctly performed, this torsion test has the main advantage of inducing fracture by torsion in the reduced hourglass shaped joined section, thus providing pure shear strength of the joined components with limited stress concentration nearby.

However, the brittle or ductile nature of the joining material itself has to be carefully taken into account: if the joining material is purely brittle, such as glasses or glass-ceramics, results obtained by using the maximum (and final) point of the torsion curve (torsional moment versus torsion angle) to calculate the shear strength are correct.

On the contrary, if the joining material is ductile, such as adhesives or brazing alloys, shear strength results obtained as above are wrong: the torsion curves may be very different when fully joined or ring-shaped hourglass joined samples are tested. A difference of about 100% was measured with torsion tests on Araldite AV119 fully joined samples compared to ring-shaped ones [15]. The difference is due to the wrong use of the maximum torsional moment in the torsion curve to calculate the shear strength of these joined samples: in the case of ductile joining materials, the curve shows a nonlinear-plastic behaviour. In order to use the torsion curve maximum point to calculate shear strength, the curve must be linear elastic only.

The aim of this paper is two-fold: first, to provide designers with reliable, pure shear strength and elastic properties (elastic modulus and Poisson's ratio) for an epoxy joined glass-to-steel component; second, to propose a method to obtain these important data in case of an unknown brittle or plastic behaviour of the adhesive.

An example of glass-to-steel adhesive joined component used in buildings is shown in Fig. 1: a structure including glass panels was built in 2015 at the University of Palermo, Italy, by adhesive joining of glass to steel, with a joint configuration similar to the one subject of this paper.

2. Materials and method

An epoxy adhesive EPX DP490 (3 M™ Scotch-Weld™) supplied as a paste was used as joining material for soda-lime glass slabs ($50 \times 50 \times 10$ mm^3) and AISI304 steel samples of different size and shape (Fig. 2).

Steel surfaces to be joined were polished by SiC grit paper (P1000) then ultrasonic cleaned with acetone before joining. Both as received and etched glass slabs were joined to steel. Glass etching was done by hydrofluoric acid (HF, 40%, Sigma-Aldrich): HF droplets were dropped on the glass surface to be joined (5 to 15 min), then rinsed with distilled water and dried with compressed air [22].

To manufacture the joints, a thin layer of adhesive was manually placed between the two adherends: particular attention was paid to control and avoid the formation of adhesive spew fillets. Samples were placed in suitable sample holders and loaded with about 1 kPa during the whole curing time to keep them in the correct position during curing, done at room temperature for seven days, according to the adhesive datasheet. The thickness of each joint, ranging between 100 μm and 150 μm, was calculated *ex-post* by measuring the difference of the sample height before and after joining [23].

With the aim of measuring the mechanical behaviour of the joints under shear stress, full joined steel hourglass (SSfHG, Fig. 2a), ring-

Fig. 1. Example of building with glass and steel: particular of the glass panel with the adhesive joint glass/steel.

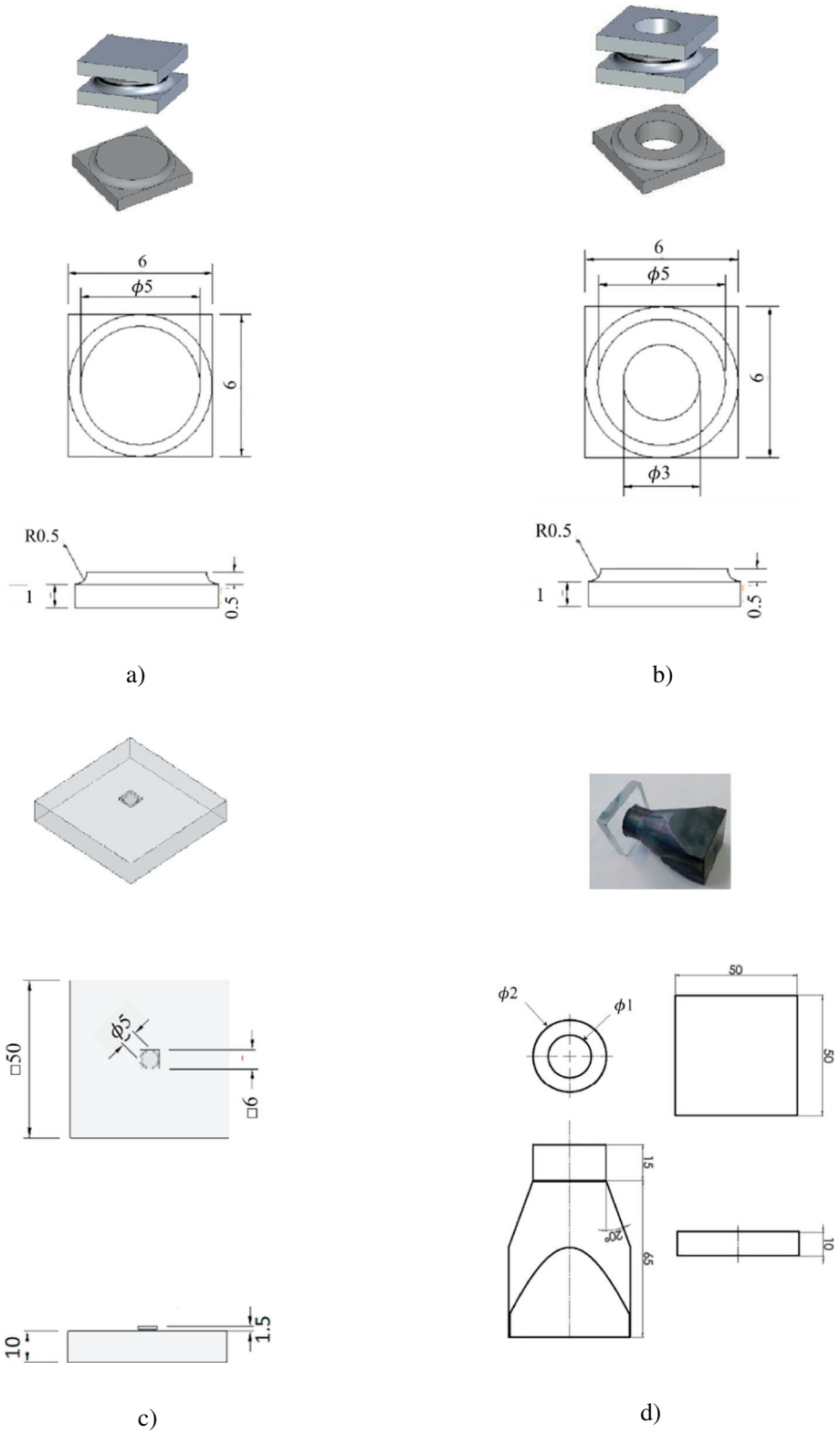

Fig. 2. Size and shape of joined samples tested in torsion: a) full joined steel hourglass (Steel-Steel-full-joined-HourGlass, SSfHG); b) ring-shaped steel hourglass (Steel-Steel-ring-shaped-HourGlass, SSrHG); c) half hourglass joined to a glass plate (Steel-Glass-half-HourGlass, SGhHG); d) full-scale ($\phi_2 = 30$ mm) ring-shaped steel fixture joined to a glass plate (Steel-Glass-ring-shaped-Full-Scale, SGrFS, with diameter ratios $\phi_1/\phi_2 = 0.40, 0.53, 0.67, 0.80$).

shaped steel hourglass (SSrHG, Fig. 2b) and half hourglass joined to a glass slab (SGhHG, Fig. 2c) were prepared and tested (at least five samples per type) at room temperature. Size and shape of the joined hourglasses in Fig. 2a have been described and their behaviour in torsion has been modelled in [19].

Full-scale joint tests (similar to the real component in Fig. 1) were performed on a 30 mm (outer diameter) ring-shaped steel component joined to a glass slab (SGrFS, Fig. 2d), with diameter ratios of 0.40, 0.53, 0.67, and 0.80, respectively.

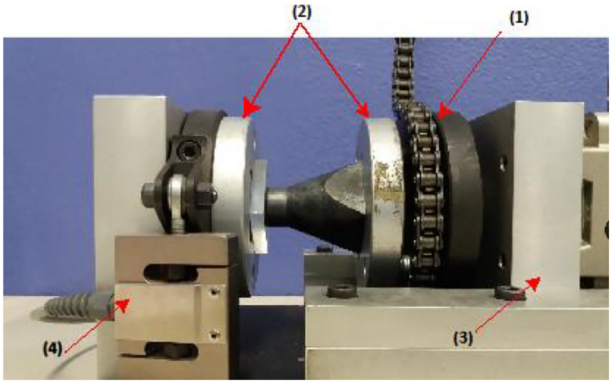

Fig. 3. Torsion test set up with the full-scale ring-shaped steel fixture joined to a glass plate and ready to be tested.

Fig. 3 shows the home-built apparatus used to perform torsional tests. In particular, it is possible to identify the load transmission chain (1), the sample grips (2), the chassis of the torsion apparatus (3) and a 2 kN load-cell (4). The torsion apparatus was coupled with a Universal Testing Machine Zwick-Roell Z100 (Germany) setting a constant cross-head speed to 0.5 mm/min corresponding to about 0.65 degree/min.

The shear strength of bars of the same steel joined by the same adhesive (joined sample size: 36 mm × 3 mm × 4 mm) was also measured at room temperature on five samples with A4PB tests (ASTM C1469 [15]), using a universal testing machine SINTEC D/10 with suitable fixtures and cross-head speed of 0.3 mm/min.

The peak load P_{max} was recorded for each test and the shear strength (τ_J) was calculated with Eq. (1), according to the ASTM C1469 [15]:

$$\tau_J = Shear\ Strength = \frac{P_{max}(S_o - S_i)}{A(S_o + S_i)} \quad (1)$$

where $A = 4\ mm \times 3\ mm = 12\ mm^2$ is the cross section, $S_o = 30$ mm is the outer span, and $S_i = 4$ mm is the inner span.

All samples fractured in the joined region. After mechanical tests, the fracture surfaces were observed by optical microscopy to determine their adhesive or cohesive failure mode.

The elastic modulus of the adhesive inside the joined area and as bulk material was measured in triplicate by nano-indentation technique, using the Continuous Stiffness Measurement (CSM) method with a Berkovich indenter [24]. The elastic modulus was continuously measured up to the fixed maximum penetration depth of 1500 nm. The fixed distance of 50 μm was kept between the individual indents from all sides. The elastic modulus results measured by indentation were compared with the elastic modulus obtained by Impulse Excitation Technique (IET, ASTM E-1876 [25]) on the adhesive bulk samples (2 mm × 3 mm × 25 mm) cured with the same curing protocol of the joined samples (room temperature, seven days, in triplicate).

3. Results

The EPX DP490 adhesive (3M™ Scotch-Weld™) lap-shear strength reported on the datasheet and obtained according to BS 5350-C5 [26] on etched aluminium joined samples at room temperature is about 30 MPa. No data are provided for steel-to-steel or steel-to-glass joints.

According to the datasheet, this bi-component epoxy adhesive is a "*black, thixotropic, gap filling adhesive, designed for use where toughness and high strength are required*".

However, a brittle behaviour of this adhesive has been reported in [27], after lap-shear test on joined glass slabs: all joints failed with a brittle failure starting inside the adhesive and propagating inside the glass. No plastic deformation was measured in [27] for this adhesive and its average lap-shear strength was about 19 MPa, but as the authors correctly pointed out, this value is referred to the "*adhesive shear strength governed by glass failure*".

This is a typical problem arising with lap-shear tests where singularities due to the sample geometry (i.e., sharp edge of the adherend) and the presence of interfaces (i.e., adhesive/glass and adhesive/steel) induce stress concentration thus causing premature failure of the adherend [28].

Torsion tests on full joined hourglass samples (SSfHG in Fig. 2a) were modelled and demonstrated to be appropriate to measure the pure shear strength in case of brittle adhesives [19,21]: in this case, the last (maximum) point of the torsion curve can be used to calculate the shear strength of the joint, providing that the fracture starts and propagates inside the joined area. If this is the case, the result obtained is the pure shear strength of the joined sample, without other spurious stresses (e.g. bending, tensile, peeling) involved.

However, if the adhesive is not purely brittle, full joined hourglass torsion curves show a certain nonlinear behaviour due to the adhesive plasticity and the maximum value of the torsion curve cannot be used to calculate the joint shear strength. In this paper, we propose an experimental way to obtain a pure linear behaviour, by using ring-shaped joined samples. The diameter ratio of the ring-shaped sample must be increased until a linear behaviour is obtained.

Several configurations of steel-to-steel and steel-to-glass joints were tested in torsion. Since it was impossible to obtain hourglass-shaped glass samples, it was decided to start testing steel-to-steel hourglasses.

Torsion curves, together with representative fracture surfaces are shown in Figs. 4–6. Curves are plotted from the onset of a steep increment of the torsional moment, immediately after an initial phase where the backlash inside the load transmission chain is fully compensated. Fig. 4 is referred to full joined (Fig. 4a) and 1 mm width ring-shaped (Fig. 4c) steel hourglass samples, their size reported in Fig. 2a and b. All fracture surfaces showed a mixed adhesive/cohesive fracture mode with adhesive on both surfaces after fracture and their typical morphology is reported in Fig. 4b and d. It is worth noting that a nonlinear behaviour before fracture ("plateau") is more evident for full joined samples than for ring-shaped ones, as expected for a ring-shaped geometry. This is due to a certain plasticity of the adhesive, even though it is defined as brittle in [27] after lap-shear test. A higher reproducibly of results is evident for the ring-shaped configuration: three out of four curves are almost overlapped, but they still show a certain plastic behaviour before fracture, and they are thus unsuitable to calculate the shear strength by using their maximum value.

Since it is practically impossible to join and test lower than 1 mm width ring-shaped hourglasses of this size, a different configuration was tested, with size shown in Fig. 2c, and results in Fig. 5a. This was also a way to test steel-to-glass joints with hourglass geometry: *only one half* of the steel hourglass was joined to glass slabs (Fig. 2c). We selected the full joined hourglass and not the ring-shaped one, because it is experimentally very difficult to have the adhesive on the ring-shaped surface only, when such a tiny specimen is pushed on the glass slab for joining. Mechanical removal of spew fillets in this case was considered detrimental to the quality of the joint itself.

The torsion curves, together with their representative fracture surfaces, are shown in Fig. 5.

Mixed adhesive/cohesive failures were again obtained, with most of the black adhesive visible on the glass surface, thus suggesting a stronger adhesive/glass interface than the adhesive/steel one. As in the previous cases (Fig. 4), a nonlinear-plastic behaviour before fracture is evident in Fig. 5a.

A remarkably increased strength was measured when the steel half hourglasses where joined to etched glass slabs (Fig. 5c and d), with the majority of the adhesive on the glass side. Even though in this case it was also not possible to measure the joint shear strength due to a certain plastic behaviour of the curve, it is worth noticing that this torsion test is able to detect an increased torsional resistance of the joint when the glass surface is properly etched (Fig. 5e): the plateau ranges

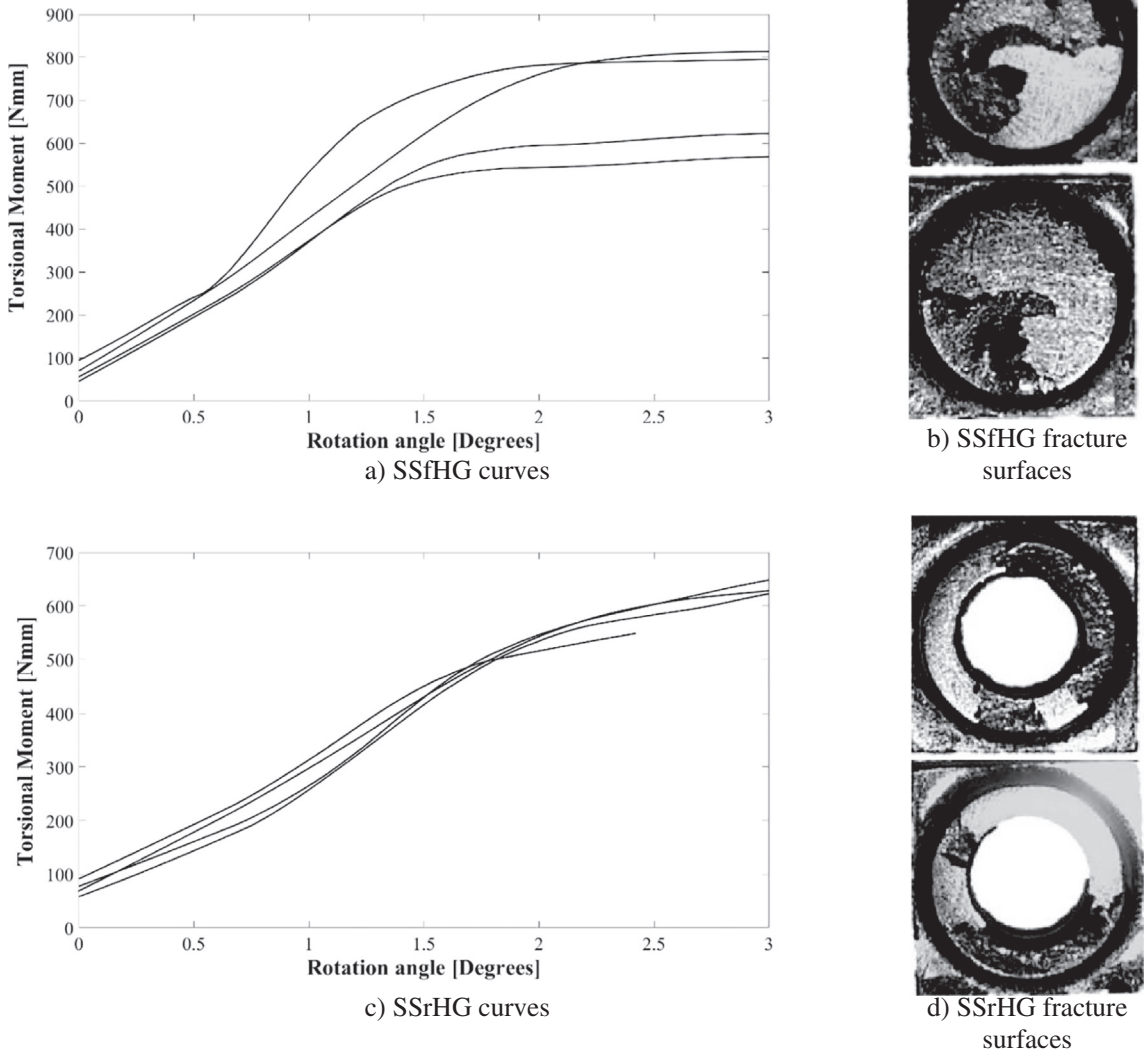

Fig. 4. Torsion versus angle curves (a and c) and representative fracture surfaces (b and d) of full joined (a and b), and ring-shaped (c and d) steel hourglasses after torsion test surfaces (adhesive is black).

between 800 and 1000 Nmm with etched glass (Fig. 5c), while for non-etched ones is 650–750 Nmm only (Fig. 5a).

Even though etching seems to be effective to increase the shear strength of these joints, it must be considered that glass etching, like any other type of glass surface roughening, results in a reduction of the glass strength, which is disadvantageous in the design of structural glass components and must be properly tested.

A negligible increase in torsional strength was measured in case of a 5 minute etching (Fig. 5f), compared to the non-etched ones and curves are not reported here.

In order to obtain a linear only torsion curve and to measure the shear strength for full-scale glass-to-steel joints, some ring-shaped steel samples close to the real geometry (30 mm outer diameter), with a ring-shaped joined area having ring width of 9, 7, 5 and 3 mm (Fig. 2d) were joined with the same adhesive to the same glass slabs and tested in torsion. Resulting torsion curves, together with representative fracture surfaces, are shown in Fig. 6.

The option of testing a full joined steel fixture of 30 mm diameter to glass plates was discarded, due to the too high torque necessary to break it, unsuitable for this torsion equipment.

Torsion tests on steel fixtures with ring width of 9 and 7 mm caused indeed the fracture inside the glass on most of samples and curves are not reported here. Similar undesired failures were observed in other three tests on fixtures with ring width of 3 and 5 mm and are not reported in Fig. 6a and b. For both ring widths, the fracture was mostly a mixed type adhesive-cohesive as observed before.

A nonlinear behavior is still visible in the curves related to the fixture with ring width of 5 mm (Fig. 6b), whereas nonlinearity disappears in the curves related to the fixture with ring width of 3 mm (Fig. 6a).

In Fig. 7a the asymmetrical four-point bending test (A4PB) setup is shown, where S_i is the inner span pin distance (4 mm), S_o is the outer span pin distance (30 mm), and the black arrows show the forces applied.

A4PB tests were performed on steel bars (same steel) joined by the same adhesive, with the same curing: due to the difficulty of obtaining glass bars of this size, it was decided to use A4PB on steel-to-steel joints. An average shear strength of 23 $\pm$ 2 MPa was obtained. As reported in Fig. 7b, all fracture surfaces showed a mixed adhesive/cohesive fracture mode, as already observed in the torsion specimens.

In order to provide a complete range of data for modelling of these adhesively bonded glass-to-steel components, the elastic modulus of

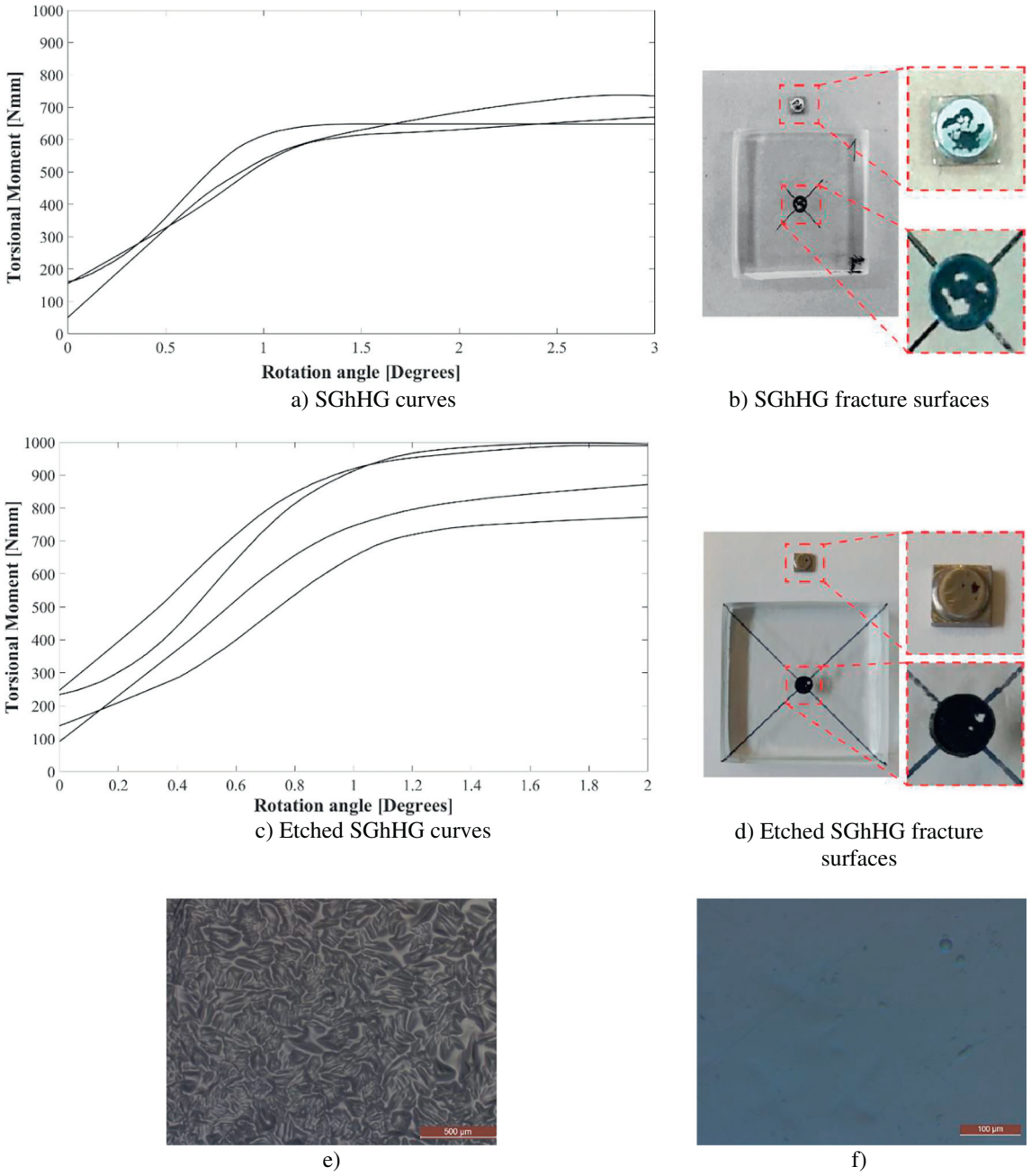

Fig. 5. Torsion versus angle curves (a and c) and representative fracture surfaces (b and d) of glass plates joined to steel half hourglasses after torsion test: as received glass (a and b) and HF etched glass (c and d). Optical microscopy of HF etched glass, 15 min (e) and 5 min (f).

the adhesive was measured by nano-indentation technique both in the joined area and in the adhesive as a bulk specimen.

An Impulse Excitation Technique (IET) was also used to measure the elastic modulus of the adhesive as a bulk, for comparison purposes: all results are summarized in Table 1.

A value of 1100 ± 100 MPa was measured when the adhesive is in the joined region (E_J in Table 1), while 1900 ± 100 MPa was measured on bulk samples of the same adhesive (E_B in Table 1), comparable to what measured by IET (2100 ± 100 MPa, $E_{B,IET}$ in Table 1). A possible explanation can be in the different arrangement of the polymeric chains during curing when they are between two surfaces or in a free, unconstrained volume.

4. Discussion

The experimental results showed that a nonlinear-plastic behaviour is present in most of the joint types. In some cases, e.g. the SSfHG and the SGhHG joints, an evident plateau revealed an extended plastic region in the torsion curve when the maximum of the torsional moment was reached. In some other cases, e.g. the SSrHG and the SGrFS with ring width 5 mm, the plateau was less evident, and in only one case, the SGrFS with ring width 3 mm, the behaviour was completely elastic, with no plastic plateau. These different responses, for the same ductile adhesive, are directly related to the joint geometry. The effect of the joint geometry on the torsion curve was approximately described by taking into account a simplified model of joint geometry and material behaviour. In particular, the different geometries were simplified into an equivalent torsion bar, with hollow cross-section and length *L*

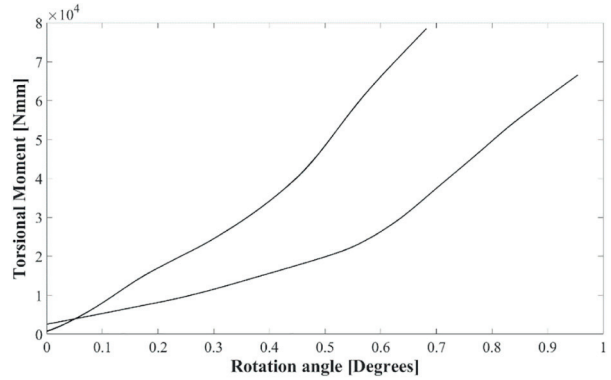

a) SGrFS curves (ϕ_1/ϕ_2 = 0.80, with ring width 3 mm)

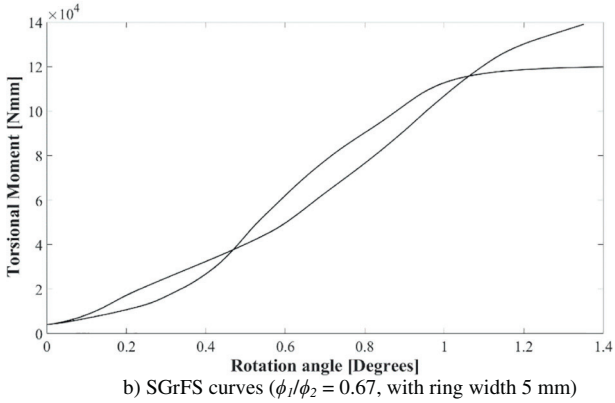

b) SGrFS curves (ϕ_1/ϕ_2 = 0.67, with ring width 5 mm)

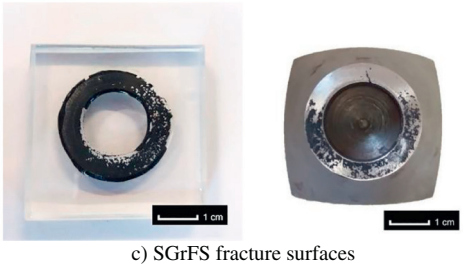

c) SGrFS fracture surfaces

Fig. 6. Torsion versus angle curves (a and b) and representative fracture surfaces (c) of full-scale (ϕ_2 = 30 mm) ring-shaped steel fixture joined to a glass plate.

(Fig. 8a and Table 2), made of the investigated adhesive. The inner and outer radii of the hollow cross-section were directly taken from the joint geometries in Fig. 2. The length L was instead estimated to have a torsional stiffness of the equivalent bar that matched the stiffness of the tested joints (Figs. 4–6).

The material behaviour of the adhesive was approximately assumed elastic-perfectly plastic (Fig. 8b), with shear modulus G equal to 393 ± 36 MPa ($G = E_J/(2(1+\nu))$, being $E_J = 1100 \pm 100$ MPa and $\nu = 0.4$ the material parameters in Table 1) and elastic limit τ_{el} equal to 23 ± 2 MPa (from A4PB tests) in case of non-etched joints (Table 2).

For the etched joints, the median elastic limit $\tau_{el,\ med}$ (equal to 29 MPa, Table 2) was estimated in order to have the modelled plastic plateau that matched the mean experimental plateau of the etched SGhHG joints (Fig. 5c).

Fig. 9 compares the experimental curves with those obtained with the simplified model of the equivalent torsion bar (Fig. 8).

As shown in Fig. 9, the modelled curves overlap the scatter bands associated to the experimental curves, in all cases. Even though strong simplifications were behind the equivalent torsion bar, Fig. 9 shows that it can be usefully exploited to explain the different torsion responses for the tested joint geometries. Moreover, the simplified model also permitted an approximate estimation of the enhancement

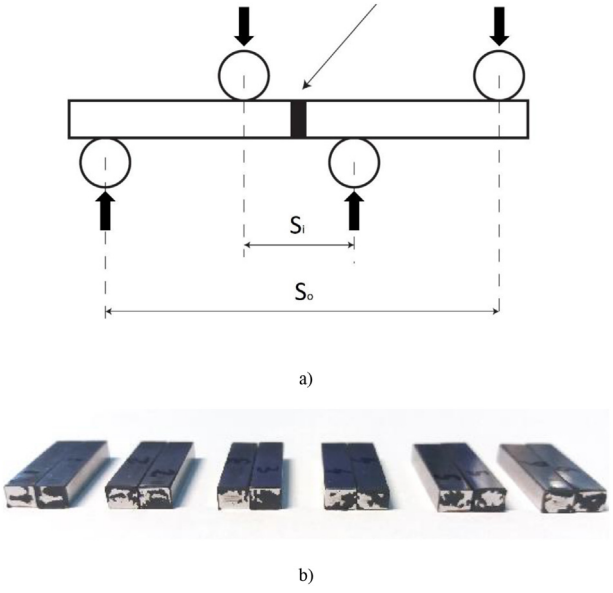

a)

b)

Fig. 7. Asymmetrical four-point bending test (A4PB) setup (a), and fracture surfaces after test on adhesive joined steel bars (b).

induced by the etching process (Fig. 9d), which increased the median elastic limit $\tau_{el,\ med}$ from 23 MPa to approximately 29 MPa.

The effect of the ring width in SGrFS joints was also estimated from the simplified model of the equivalent torsion bar. Fig. 10 depicts the modelled torsion curves for different ring widths in SGrFS joints.

According to Fig. 10, the smaller the ring width, the more brittle the behaviour. Furthermore, both the stiffness and the maximum torsional moment significantly decrease with the ring width. These considerations can be helpful when designing the SGrFS joint: for a given outer diameter, the ring width must be properly chosen in order to avoid unexpected failures in the glass slab and to have an immediate estimation of the torsional shear strength of the ductile adhesive. Table 3 reports, for different ring widths of the SGrFS joint, the errors made when estimating the torsional shear strength from the simple linear elastic torsion formula:

$$\tau_{MAX} = \frac{16 M_{t,\ MAX}}{\pi \phi_2^3 \left(1-(\phi_1/\phi_2)^4\right)} \tag{2}$$

where $M_{t,\ MAX}$ is the maximum torsional moment, ϕ_1 and ϕ_2 are the inner and outer diameters.

Table 3 shows that the error decreases with the ring width and it becomes acceptable only if the ring width is below 2 mm (i.e., the estimated torsional shear strength is within the scatter band observed with A4PB tests). Nonetheless, the experimental scatter of these kinds of torsion tests should be carefully controlled through an accurate joint preparation, to avoid too much scattered results as those shown in Fig. 9e. In this respect, it is expected that, thanks to a more limited extension of the adhesive region and to a smaller maximum torsional moment (which means less probability of having unexpected failures in the

Table 1
Elastic properties of the adhesive measured on bulk adhesive and inside the joint by nano-indentation and Impulse Excitation Technique (IET) as indicated.

	Nanoindentation		IET
Poisson's ratio ν	E_J	E_B	$E_{B,IET}$
	[MPa]	[MPa]	[MPa]
0.40	1100 ± 100	1900 ± 100	2100 ± 100

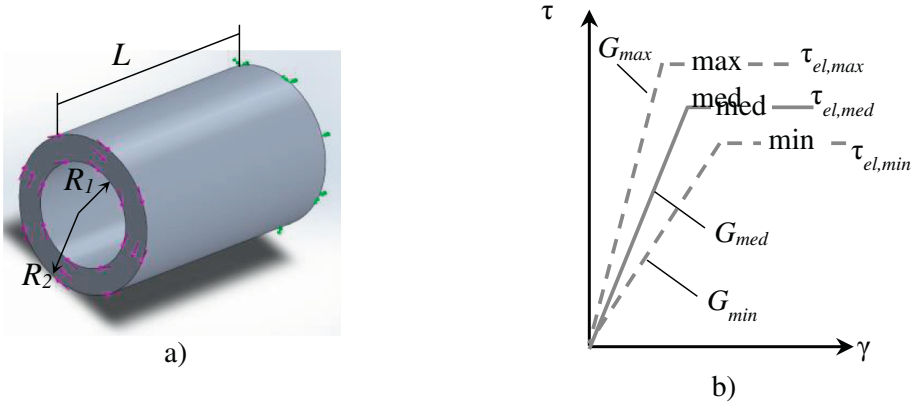

Fig. 8. Equivalent torsion bar: a) geometric model; b) material model.

glass slab), the experimental scatter should significantly reduce in case of SGrFS joints with 1 mm ring width.

5. Conclusions

The aim of the paper was to provide designers with reliable shear strength and elastic properties for an epoxy joined glass-to-steel component: torsional shear strength and elastic properties of an adhesively bonded glass-to-steel component were measured on several configurations in order to obtain pure shear strength results.

An epoxy resin adhesive EPX DP490 (3 M™ Scotch-Weld™ Epoxy Adhesive) was used as joining material for AISI304 steel and soda-lime glass. Several steel-to-steel and steel-to-glass joined samples were tested in torsion and asymmetrical four-point bending. Torsion curves showed an evident nonlinear plastic behaviour in almost all cases. Finally, the full-scale steel component joined to a glass slab provided a quasi-linear behaviour, when the width of the ring-shaped steel component was reduced to 3 mm.

The elastic modulus of the adhesive was measured by nano-indentation technique both in the joined area and in the adhesive as a bulk specimen, giving 1100 ± 100 MPa and 1900 ± 100 MPa, respectively. An impulse excitation technique used to measure the bulk adhesive elastic modulus, for comparison purposes, measured a consistent 2100 ± 100 MPa, thus suggesting a lower elastic modulus for the adhesive when constrained in a joint.

A simplified equivalent torsion bar made of an elastic-perfectly plastic material was also considered to model the ductile-brittle behaviour of the adhesive joints. The simplified model was in good agreement with the experimental data and permitted to estimate the positive effect of the etching process made on glass slabs before joining to steel.

The two main findings of this work are the following: i) when the joining material is not purely brittle, several *ring shaped joined samples with decreasing ring width should be prepared and tested*, until a purely linear behaviour of the torsion curve versus angle curve is obtained, *to obtain the shear strength*; ii) when the adhesive is *inside* the joined volume, its elastic modulus may be lower than what measured on a bulk, un-constrained adhesive.

Table 2
Numeric data used for the equivalent torsion bar.

Joint type	$R_2^{(1)}$ [mm]	$R_1^{(1)}$ [mm]	$L^{(2)}$ [mm]	τ_{el} [MPa]	$G^{(5)}$ [MPa]
SSHG	2.5	0	1.10	23 ± 2[3]	393 ± 36
SSrHG	2.5	1.5	1.35	23 ± 2[3]	393 ± 36
Non-etched SGhHG	2.5	0	0.65	23 ± 2[3]	393 ± 36
Etched SGhHG	2.5	0	0.65	29[4]	393 ± 36
SGrFS 3 mm	15	12	4.00	23 ± 2[3]	393 ± 36
SGrFS 5 mm	15	10	4.00	23 ± 2[3]	393 ± 36

Notes: [1] From joint geometries; [2] Estimated from experimental stiffness; [3] Elastic limit from asymmetrical four-point bending (A4PB) tests; [4] Median value, estimated from experimental data; [5] Shear modulus from nanoindentation tests.

Data availability

- The raw/processed data required to reproduce these findings cannot be shared at this time due to technical or time limitations.
- The raw/processed data required to reproduce these findings cannot be shared at this time as the data also forms part of an ongoing study.

CRediT authorship contribution statement

Stefano De La Pierre: Conceptualization, Project administration, Visualization, Data Curation, Investigation. **Tommaso Scalici:** Visualization, Data Curation, Investigation. **Peter Tatarko:** Funding acquisition, Data Curation. **Antonino Valenza:** Supervision, Funding acquisition, Project administration, Resources. **Luca Goglio:** Supervision, Funding acquisition, Methodology, Formal analysis. **Davide S. Paolino:** Visualization, Data Curation, Investigation, Methodology, Formal analysis. **Monica Ferraris:** Conceptualization, Supervision, Funding acquisition, Project administration, Resources.

Declaration of competing interest

The authors declare that they have no known competing financial interests or personal relationships that could have appeared to influence the work reported in this paper.

Acknowledgements

One of the authors (S.DLP) would like to thank KMM-VIN for providing him the Research Fellowship 2017. (P.T.) gratefully acknowledges the financial support of the Slovak Research and Development Agency under the contract No. APVV-17-0328.

This research has been partially funded by: VESTRA – "Elementi strutturali in VEtro STRAtificato per applicazioni in ingegneria civile" – PO FESR Regione Siciliana 2007-2013, Italy.

All the materials for this work were provided and machined by NeriGlass s.r.l., Italy, within the research program "VESTRA - Elementi Strutturali in VEtro STRAtificato per applicazioni in Ingegneria Civile" coordinated by the University of Palermo, Italy.

This activity was partially developed in the frame of J-TECH@POLITO (Advanced Joining Technology at Politecnico di Torino; www.j-tech.polito.it).

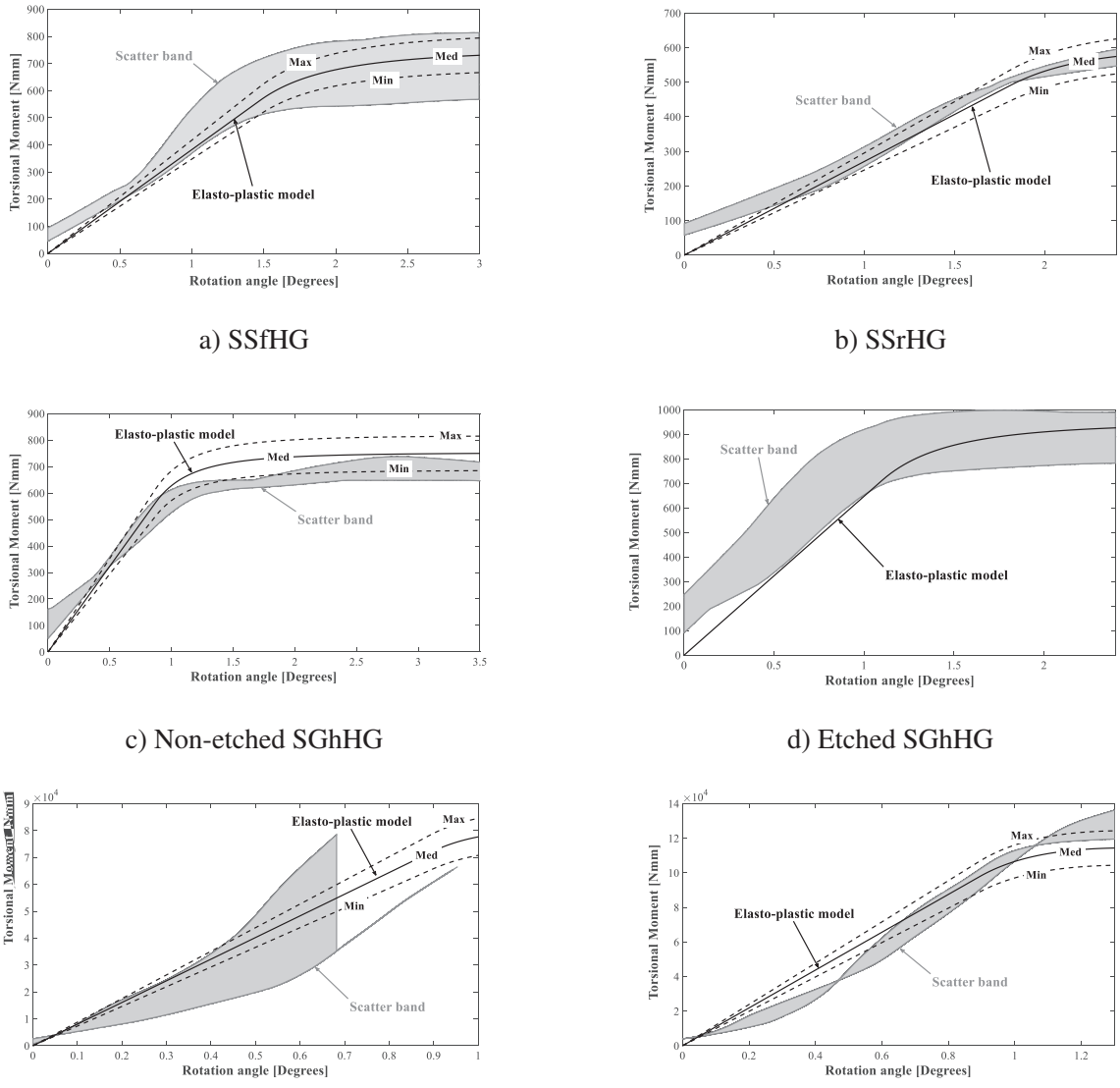

a) SSfHG

b) SSrHG

c) Non-etched SGhHG

d) Etched SGhHG

e) SGrFS, with ring width 3 mm

f) SGrFS, with ring width 5 mm

Fig. 9. Comparison between experimental torsion curves (grey band) and analytically modelled torsion curves (minimum and maximum curves with dashed lines and median curve with solid line): a) SSfHG joint; b) SSrHG joint; c) Non-etched SGhHG joint; d) Etched SGhHG joint (the solid line refers to the predicted median curve); e) SGrFS joint with ring width 3 mm; f) SGrFS joint with ring width 5 mm.

References

[1] F. Pariafsai, A review of design considerations in glass buildings, Front. Archit. Res. 5 (2016) 171–193, https://doi.org/10.1016/j.foar.2016.01.006.

[2] F. Marchione, P. Munafò, Experimental strength evaluation of glass/aluminum double-lap adhesive joints, J. Build. Eng. 30 (2020), 101284. https://doi.org/10.1016/j.jobe.2020.101284.

[3] V. Fiore, L. Calabrese, E. Proverbio, G. Galtieri, T. Scalici, V.M. Lo Presti, et al., Pull-off adhesion of hybrid glass-steel adhesive joints in salt fog environment, J. Adhes. Sci. Technol. 30 (2016)https://doi.org/10.1080/01694243.2016.1178018.

[4] J.R. Vinson, Adhesive bonding of polymer composites, Polym. Eng. Sci. 29 (1989) 1325–1331, https://doi.org/10.1002/pen.760291904.

[5] C. Sarrado, A. Turon, J. Costa, J. Renart, On the validity of linear elastic fracture mechanics methods to measure the fracture toughness of adhesive joints, Int. J. Solids Struct. 81 (2016) 110–116, https://doi.org/10.1016/J.IJSOLSTR.2015.11.016.

[6] M. Heshmati, R. Haghani, M. Al-Emrani, Dependency of cohesive laws of a structural adhesive in Mode-I and Mode-II loading on moisture, freeze-thaw cycling, and their synergy, Mater. Des. 122 (2017) 433–447, https://doi.org/10.1016/j.matdes.2017.03.016.

[7] F.M. González Ramírez, F.P. Garpelli, R.C.M. Sales, G.M. Candido, M.A. Arbelo, M.Y. Shiino, M.V. Donadon, Experimental characterization of Mode I fatigue delamination growth onset in composite joints: a comparative study, Mater. Des. 160 (2018) 906–914, https://doi.org/10.1016/j.matdes.2018.10.007.

[8] K. Machalická, M. Eliášová, Adhesive joints in glass structures: effects of various materials in the connection, thickness of the adhesive layer, and ageing, Int. J. Adhes. Adhes. 72 (2017) 10–22, https://doi.org/10.1016/j.ijadhadh.2016.09.007.

[9] T. Scalici, G. Pitarresi, G. Catalanotti, F.P. van der Meer, A. Valenza, The Transverse Crack Tension test revisited: an experimental and numerical study, Compos. Struct. 158 (2016)https://doi.org/10.1016/j.compstruct.2016.09.033.

[10] ASTM, ASTM D7905/7905M - 14 - Standard Test Method for Determination of the Mode II Interlaminar Fracture Toughness of Unidirectional Fiber-Reinforced Polymer Matrix Composites, 2014.

[11] International Organization for Standardization, ISO 15114:2014 - Fibre-Reinforced Plastic Composites – Determination of the Mode II Fracture Resistance for Unidirectionally Reinforced Materials Using the Calibrated End-Loaded Split (C-ELS) Test and an Effective Crack Length Approach, 2014.

[12] ASTM. ASTM D905-08(2013) - Standard Test Method for Strength Properties of Adhesive Bonds in Shear by Compression Loading.

[13] G. Viana, J. Machado, R. Carbas, M. Costa, L.F.M. da Silva, M. Vaz, M.D. Banea, Strain rate dependence of adhesive joints for the automotive industry at low and high temperatures, J. Adhes. Sci. Technol. 32 (19) (2018) 2162–2179, https://doi.org/10.1080/01694243.2018.1464635.

[14] S.K. Gupta, D.K. Shukla, Effect of stress rate on shear strength of aluminium alloy single lap joints bonded with epoxy/nanoalumina adhesives, Int. J. Adhes. Adhes. 99 (2020), 102587. https://doi.org/10.1016/j.ijadhadh.2020.102587.

[15] ASTM. ASTM C1469-10, Standard Test Method for Shear Strength of Joints of Advanced Ceramics at Ambient Temperature 2015, 2015.

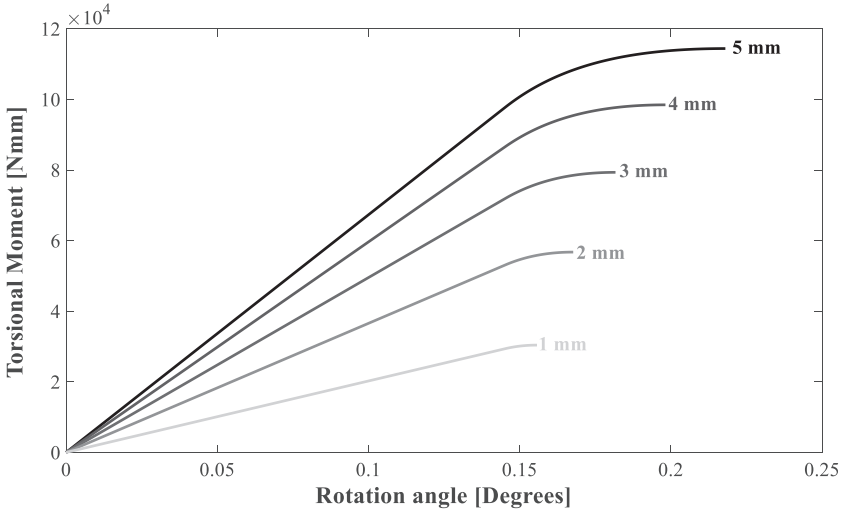

Fig. 10. Modelled torsion curves for different ring widths in SGrFS joints.

[16] M. Ferraris, A. Ventrella, M. Salvo, M. Avalle, F. Pavia, E. Martin, Comparison of shear strength tests on AV119 epoxy-joined carbon/carbon composites, Compos. Part B Eng. 41 (2010) 182–191, https://doi.org/10.1016/j.compositesb.2009.10.008.
[17] T. Osipova, J. Wei, G. Pećanac, J. Malzbender, Room and elevated temperature shear strength of sealants for solid oxide fuel cells, Ceram. Int. 42 (2016) 12932–12936, https://doi.org/10.1016/j.ceramint.2016.05.064.
[18] M. Ferraris, M. Salvo, V. Casalegno, M. Avalle, A. Ventrella, Torsion tests on AV119 epoxy - joined SiC, Int. J. Appl. Ceram. Technol. 9 (2012) 795–807, https://doi.org/10.1111/j.1744-7402.2011.02740.x.
[19] L. Goglio, M. Ferraris, Bonding of ceramics: an analysis of the torsion hourglass specimen, Int. J. Adhes. Adhes. 70 (2016) 46–52, https://doi.org/10.1016/J.IJADHADH.2016.05.006.
[20] T. Nozawa, H. Ogiwara, J. Kannari, H. Kishimoto, H. Tanigawa, Torsion test technique for interfacial shear evaluation of F82H RAFM HIP-joints, Fusion Eng. Des. 86 (2011) 2512–2516, https://doi.org/10.1016/j.fusengdes.2011.01.110.
[21] M. Ferraris, A. Ventrella, M. Salvo, D. Gross, Shear strength measurement of AV119 epoxy-joined SiC by different torsion tests, Int. J. Appl. Ceram. Technol. 11 (2014) 394–401, https://doi.org/10.1111/ijac.12025.
[22] C. Iliescu, J. Jing, F.E.H. Tay, J. Miao, T. Sun, Characterization of masking layers for deep wet etching of glass in an improved HF/HCl solution, Surf Coat. Tech. 198 (2005) 314–318, https://doi.org/10.1016/j.surfcoat.2004.10.094.
[23] J.J.G. Oliveira, R.D.S.G. Campilho, F.J.G. Silva, E.A.S. Marques, J.J.M. Machado, L.F.M. da Silva, Adhesive thickness effects on the mixed-modefracture toughness of bonded joints, J Adhes. 96 (1–4) (2020) 300–320, https://doi.org/10.1080/00218464.2019.1681269.
[24] X. Li, B. Bhushan, A review of nanoindentation continuous stiffness measurement technique and its applications, Mater. Charact. 48 (2002) 11–36, https://doi.org/10.1016/S1044-5803(02)00192-4.
[25] ASTM. ASTM E1876 2015 Standard Test Method for Dynamic Young's Modulus, Shear Modulus, and Poisson's Ratio by Impulse Excitation of Vibration. 2015
[26] BSI. BS 5350-C5:2002 Methods of Test for Adhesives. Determination of Bond Strength in Longitudinal Shear for Rigid Adherends.
[27] S. Nhamoinesu, M. Overend, The mechanical performance of adhesives for a steel-glass composite façade system, Challenging Glas. 3 Conf. Archit. Struct. Appl. Glas. CGC 2012 2012, pp. 293–306, https://doi.org/10.3233/978-1-61499-061-1-293.
[28] D.M. Gleich, M.J.L. Van Tooren, A. Beukers, Analysis and evaluation of bondline thickness effects on failure load in adhesively bonded structures, J. Adhes. Sci. Technol. 15 (2001) 1091–1101, https://doi.org/10.1163/156856101317035503.

Table 3
Effect of ring width on the estimation of the torsional shear strength from SGrFS joints.

Ring width [mm]	$M_{t,MAX}$ [Nmm]	τ_{MAX} [MPa]	Error
5	114×10^3	26.9	16.9%
4	98.5×10^3	26.1	13.6%
3	79.3×10^3	25.3	10.2%
2	57.7×10^3	24.6	6.8%
1	30.4×10^3	23.8	3.4%